TRENDS IN SCIENCES 2025; 22(12): 10862
https://doi.org/10.48048/tis.2025.10862 RESEARCH ARTICLE

Therapeutic Potential of Muli Banana Peel Extract on Modulating Inflammation, Proliferation, and Apoptosis in A Rat Model of Endometriosis

Siti Maesaroh[1,5,*], Soetrisno[1,2], Harijono Kario Sentono[1,3] and Dono Indarto[1,4]

[1]*Doctoral Program of Medical Sciences, Faculty of Medicine, Universitas Sebelas Maret, Surakarta, Indonesia*
[2]*Department of Obstetrics and Gynecology, Faculty of Medicine, Universitas Sebelas Maret, Surakarta, Indonesia*
[3]*Dermatology and Venereology Department, Universitas Sebelas Maret, Surakarta, Indonesia*
[4]*Department of Physiology and Biomedical Laboratory, Faculty of Medicine, Universitas Sebelas Maret, Surakarta, Indonesia*
[5]*Midwifery Study Program, Faculty of Health Sciences, Aisyah University Pringsewu, Lampung, Indonesia*

([*]Corresponding author's e-mail: siti_maesaroh@student.uns.ac.id)

Received: 6 June 2025, Revised: 20 June 2025, Accepted: 27 June 2025, Published: 30 August 2025

Abstract

Endometriosis is a condition characterized by the growth of tissue resembling the endometrium outside the uterine cavity, which can lead to inflammation, pelvic pain, and infertility. *Muli* Banana Peel Extract (MBPE) derived from *Musa acuminata* Colla has demonstrated therapeutic potential in the management of endometriosis. The study aims to establish MBPE as a natural therapeutic agent for endometriosis by targeting inflammation (TNFα), cell proliferation (Ki-67, BCL2), and apoptosis (Caspase 3), while also assessing its impact on lesion regression. An experimental laboratory study with a pre-posttest-only control group design for the TNFα parameter and a posttest-only control group design for other parameters was conducted using 48 Wistar rats with an autologous endometriosis model. The rats were randomly divided into 6 treatment groups (n = 8 per group). Changes in serum TNFα levels before and after treatment, as well as tissue levels of Ki-67, BCL2, and Caspase 3 after treatment, were analyzed using enzyme-linked immunosorbent assay (ELISA). Hematoxylin and eosin (HE) staining was used to evaluate lesion size. The results showed that MBPE at a dose of 400 mg/kg body weight (BW) significantly reduced serum TNFα levels (p = 0.024), decreased tissue levels of Ki-67 (p = 0.003), and increased tissue levels of Caspase 3 (p = 0.001). Rats receiving MBPE (400 mg/kg BW) exhibited significantly smaller lesion sizes ($p < 0.001$) compared to the control group. In conclusion, MBPE showed promising therapeutic potential for endometriosis treatment through multi-target mechanisms, effectively reducing inflammation (TNFα), inhibiting cell proliferation (Ki-67), promoting apoptosis (Caspase 3), and significantly reducing lesion size. The lack of significant BCL2 modulation indicates that MBPE may primarily target intrinsic apoptotic pathways rather than anti-apoptotic mechanisms.

Keywords: Banana peel, Inflammation, Proliferation, Apoptosis, TNFα, Ki-67, BCL2, Caspase 3, Endometriosis

Introduction

Endometriosis represents a significant challenge in reproductive health, affecting 6% - 10% of women of reproductive age worldwide. This condition is characterized by recurrent pelvic pain and infertility, which significantly reduces the quality of life for women [1,2].

Its prevalence varies based on population and diagnostic methods, ranging from 2% - 11% in asymptomatic women, 5% - 50% in infertile women, and 5% - 21% in hospitalized patients with pelvic pain. In symptomatic adolescents, the prevalence reaches 49% in cases of chronic pelvic pain and 75% in pain unresponsive to treatment [3].

As a multifactorial disease with an etiology that is not yet fully understood, the pathogenesis of endometriosis involves various theories, including

retrograde menstruation, metaplasia, oxidative stress, hormonal imbalance, immune dysfunction, and stem cell involvement [4]. Retrograde menstruation, which refers to the backflow of menstrual blood into the peritoneum followed by implantation and tissue growth, is the most widely accepted theory. However, not all women with retrograde menstruation develop endometriosis, suggesting the significant role of immune dysfunction [5,6].

During retrograde menstruation, menstrual tissue that enters the peritoneal cavity activates macrophages to secrete cytotoxic cytokines such as TNF-α, which induces apoptosis in the ectopic endometrial fragments [7]. In patients with endometriosis, higher Ki-67 expression in endometriotic lesions compared to normal endometrial tissue indicates increased cell proliferation activity, contributing to the growth and spread of lesions outside the uterus [8,9].

Women with endometriosis also have a larger population of BCL2-positive macrophages in the peritoneal fluid, in contrast to women without endometriosis who have higher levels of BAX [10]. The "immune escape" theory, related to the failure of apoptosis in endometriotic cells, also involves caspase, particularly Caspase-3, which plays a key role in this process. Serum Caspase-3 levels have been identified as a reliable predictor for measuring the severity of endometriosis [11].

The management of endometriosis is categorized based on the main symptoms, namely pain and infertility. Conventional treatments, such as progestins, combined oral contraceptives, NSAIDs, GnRH agonists, and surgical interventions, are commonly used depending on the severity and the patient's needs. However, these therapies have limitations, including side effects (spotting, weight gain, osteoporosis, and mood changes) and a high recurrence rate [3,12].

Therefore, there is a clear need to investigate alternative therapies, such as phytotherapy, which may provide therapeutic benefits with fewer adverse effects [1].

Phytotherapy utilizes medicinal plants with bioactive compounds that possess anti-angiogenic, antioxidant, and pro-apoptotic properties [1]. Recent investigations have demonstrated promising therapeutic outcomes in endometriosis management through plant-derived compounds. Wulandari *et al.* [13] demonstrated that Phyllanthus niruri extract significantly reduced inflammatory markers (IL-1β, MMP-9) and oxidative stress indicators (MDA) in murine models through the activity of tannins, flavonoids, and quercetin. Alpinumisoflavone derived from Cudrania tricuspidate effectively suppressed endometriotic cell proliferation and migration by modulating AKT, MAPK, and autophagy pathways [14]. Furthermore, Maqian essential oil treatment altered the expression of 435 proteins within complement and coagulation cascades, identifying heme oxygenase 1 and acyl-CoA 6-desaturase as potential therapeutic biomarkers [15]. These findings underscore the therapeutic potential of plant-derived compounds in endometriosis treatment through their multifaceted mechanisms of action.

This study investigates MBPE to determine whether it may serve as a natural therapeutic agent. Banana peels, traditionally considered agricultural waste, are rich in phytochemicals that may be beneficial for pharmacological applications. MBPE contains bioactive compounds such as flavonoids, phenolics, carotenoids, saponins, and tannins. These bioactive constituents have been reported to exhibit antioxidant, anti-inflammatory, immunomodulatory, and pro-apoptotic properties [16,17]. Previous studies have shown applications of MBPE in wound healing and other therapeutic contexts [18,19].

Given the limitations of current therapies and the bioactive profile of MBPE, this study aims to evaluate the effects of ethanol extract of muli banana peel in Wistar rats with endometriosis established through autologous endometrial fragment transplantation. Specifically, this research seeks to assess the impact of MBPE treatment on endometriotic lesion development, proliferation markers, inflammatory markers, and apoptotic pathways to investigate its potential role in endometriosis management.

Materials and methods

Plant material and preparation

MBPE was obtained from banana peels sourced from a commercial plantation located in the Tanggamus region, Lampung Province, Indonesia. The banana peels were collected 7 days post-fruit ripening, approximately 3 months after the flowering stage. Following harvest, the bananas were subjected to controlled ripening in a shaded, well-ventilated environment for seven days

until the peels developed characteristic yellow coloration with distinct brown speckles. Subsequently, the fruits were manually separated from their peels.

The collected peels underwent preliminary processing involving thorough washing with running tap water, followed by drainage and controlled drying in a convection oven maintained at 30 - 40 °C for 24 - 30 h. The dried simplicia was mechanically ground using a laboratory mill and subsequently sieved through a 40-mesh screen to obtain uniform particle size distribution. The processed powder was then weighed and stored under appropriate conditions.

The extraction procedure was conducted at the Extract Standardization Laboratory, Faculty of Pharmacy, Universitas Muhammadiyah Surakarta, Central Java, Indonesia, employing a sequential maceration technique with 96% ethanol as the extraction solvent. A total of 500 g of banana peel powder was subjected to maceration using 96% ethanol at a solvent-to-sample ratio of 1:10 (w/v), corresponding to 5 L of ethanol per extraction cycle. The maceration process was maintained for 3 days under ambient conditions, followed by vacuum filtration using a Buchner funnel apparatus. The resulting filtrate was concentrated under reduced pressure to yield the 1st semi-concentrated extract (Extract 1).

The extraction procedure was repeated using the remaining ethanol to re-macerate the residual powder for an additional 3-day period, followed by filtration and concentration to produce the 2nd semi-concentrated extract (Extract 2). This process was reiterated for a third cycle to generate the third semi-concentrated extract (Extract 3). The 3 semi-concentrated extracts were subsequently combined and subjected to final concentration using a water bath maintained at 65 °C for 62 h to obtain the concentrated MBPE.

Subsequently, LC-MS/MS-QTOF (Liquid Chromatography-Mass Spectrometry/Tandem Mass Spectrometry Quadrupole Time-of-Flight), ICP OES (Inductively Coupled Plasma Optical Emission Spectroscopy), and HPLC-PDA (High-Performance Liquid Chromatography with Photodiode Array detector) analyses were conducted at Saraswanti Indo Genetech (SIG) laboratory in Bogor, Indonesia, under reference number SIG.MARK.V.2023.010895.2 to identify the phytochemical constituents, mineral content, and vitamin content present in MBPE.

Molecular docking analysis

The *in silico* process began with the preparation of test ligands, which were downloaded from PubChem in .sdf format and then converted to .pdb format using Discovery Studio Visualizer. The ligands were subsequently geometrically optimized using Avogadro software with the MMFF94 method for 10,000 steps to obtain the most stable structure with the lowest energy.

The target protein used was the TNF Receptor (PDB ID: 1EXT), downloaded from the Protein Data Bank (RCSB PDB). The protein preparation process involved the removal of water molecules and unnecessary residues, as well as the addition of hydrogen atoms to stabilize the charges using AutoDock software.

For method validation, the native ligand was redocked into the active site of the target protein, and the RMSD was calculated (with a cut-off of <2.0 Å). Molecular docking simulations were carried out using AutoDock version 4.2.3, with parameters such as 100 LGA runs, 150 population size, and 25,000,000 evaluations. The grid box configuration was adjusted to cover the protein's binding site with dimensions of 40×40×40 Å^3 and grid spacing of 0.375 Å.

The interactions between the test ligands and the target protein were analyzed based on binding free energy (ΔG) and inhibition constant (Ki). Binding interactions were visualized using Discovery Studio Visualizer 2024 and Visual Molecular Dynamics (VMD).

Ethical approval

This study obtained ethical approval from the Research Ethics Committee of the Faculty of Medicine, Universitas Sebelas Maret, with Approval Number 233/UN27.06.11/KEP/EC/2023. The study followed standard protocols for the use of laboratory animals.

Animal care

Female Wistar rats aged 6 weeks and weighing between 150 - 250 g were obtained from the Integrated Research and Testing Laboratory (LPPT), Universitas Gadjah Mada, and used to establish an autologous endometriosis model. All rats were housed in polypropylene cages with stainless steel lids, 4 animals per cage, with wood shaving bedding and maintained

under controlled environmental conditions (12:12 h light/dark cycle, temperature 22 ± 2 °C, humidity 50% - 60%) according to their physiological and behavioral requirements. Animals received water and feed ad libitum with a 12-h preoperative fasting period established prior to surgery.

Endometriosis implants were created following the method of Amaral *et al*. [20]. Initial laparotomy was performed during the estrus cycle to induce the endometriosis model through median laparotomy with identification of the bicornuate uterus and resection of a 2 cm segment from the uterine horn. An endometrial flap measuring 0.25 cm² (5×5 mm^2) was obtained from the resected uterine segment after immersion in 0.9% saline at 4 °C for approximately 2 min, then incised longitudinally. This portion was sutured to the abdominal wall on the right side using 2 simple 6 - 0 mononylon sutures, positioned adjacent to blood vessels, ensuring that the endometrial surface was placed in contact with the peritoneum and always facing the abdominal cavity. After ensuring hemostasis and cleaning the abdominal cavity, the abdominal wall was closed in layers using continuous 3 - 0 vicryl sutures for the musculoaponeurotic layer and continuous 3 - 0 mononylon for the skin. Antibiotics were administered to prevent infection.

Rats were anesthetized using ketamine at a dose of 90 mg/kg body weight (PT. Dexa Medica, Tangerang, Indonesia) and xylazine at a dose of 10 mg/kg body weight (PT. Tekad Mandiri Citra, Bandung, Indonesia), administered via intraperitoneal injection. In this study, the 2nd laparotomy aimed at evaluating the success of model formation was performed on day 45 post-1st surgery, following the protocol of Amaral *et al.* [20] which recommends evaluation after the treatment period rather than the standard day-30 procedure. To validate this protocol, a preliminary study was conducted on 4 rats. Macroscopic and microscopic evaluation on day 30 confirmed successful formation of the endometriosis model with characteristics of endometrial tissue containing glands and/or stroma outside the uterine cavity, which served as the basis for continuing the treatment protocol until day 45.

Following the treatment, a 2nd laparotomy was performed to assess lesion size and measure the levels of TNFα, Ki-67, BCL2, and Caspase 3. The successful development of the animal model is illustrated in **Figure 1**, which shows representative macroscopic morphology of transplanted endometrial tissue forming endometriosis lesions in Wistar rats.

Figure 1 Macroscopic and microscopic overview of the experimental animal model of endometriosis.

Based on observations in **Figure 1**, the laparotomy procedure was carefully performed to ensure successful transplantation of endometrial tissue. The procedure was carried out without any mortality among the experimental rats, indicating that it was safe and well-controlled. Histological analysis revealed the presence of endometrial glands within the peritoneal tissue of the rats, confirming the implantation and growth of endometrial tissue at the peritoneal site. These findings suggest that the rat model used in this study effectively replicates key features of human endometriosis.

Treatment

MBPE doses (200, 300, 400 mg/kg BW/day) and 14-day treatment duration were selected based on preliminary dose-finding study (4 groups, n = 3/group) demonstrating optimal TNF-α reduction and lesion size decrease at 400 mg/kg. Dose selection was supported by established safety profiles from previous studies [21,22]. The 14-day duration showed significant therapeutic response and aligns with standard protocols for anti-inflammatory interventions in rodent endometriosis models.

Successfully developed endometriosis models were randomly assigned into 6 groups (n = 8/group): Normal group (NG) receiving distilled water; negative control group (NCG) with untreated endometriosis models; positive control receiving DLBS1442 (5.4 mg/200 g BW/day); and 3 MBPE groups (200, 300, 400 mg/kg BW/day). MBPE solutions were prepared using 0.5% Na-CMC as suspending agent and administered orally once daily via gavage for 14 consecutive days.

Comprehensive safety monitoring included daily behavioral observations, body weight measurements, and mortality assessment. No toxicity, behavioral changes, or mortality were observed throughout the study period. These findings confirm the established safety profile of MBPE and validate the safety margin of the selected dose range.

Measurement of biomarkers

Biomarkers related to endometriosis pathophysiology were measured using the Enzyme-Linked Immunosorbent Assay (ELISA) technique. Four specific biomarkers were selected based on their roles in endometriosis pathogenesis: TNFα as an inflammatory marker, Ki-67 as a proliferation marker, BCL2 as an anti-apoptotic marker, and Caspase-3 as a pro-apoptotic marker. Two types of ELISA assays were performed: The 1st to measure TNFα levels in serum, and the 2nd to measure Ki-67, BCL2, and Caspase-3 levels in tissue lesions.

TNFα levels were measured by collecting serum samples on day 0 (after establishing the endometriosis model) and on day 15 after treatment. Serum TNFα concentrations were assessed using an ELISA kit (Cat.no.E0764Ra; BT-LAB, Shanghai, China), following the manufacturer's instructions. For the analysis of Ki-67, BCL2, and Caspase-3, lesion tissue samples were collected on day 15 after treatment. The tissue samples were homogenized and processed according to standard protocols before analysis. The levels of Ki-67, BCL2, and Caspase-3 were determined using respective ELISA kits (Ki-67 Cat.no.E0063Ra; BCL2 Cat.no.E0037Ra; Caspase-3 Cat.no.E1648Ra, BT-LAB, Shanghai, China), following the procedures outlined by the manufacturer.

To ensure accuracy and reliability of results, each ELISA measurement was performed in duplicate, with appropriate positive and negative controls. Intra-assay and inter-assay coefficients of variation for all ELISA kits used were within acceptable ranges (<10% and <15%, respectively) according to manufacturer specifications. Standard calibration was performed for each measurement batch using standards provided in the kits. All biomarker concentrations were expressed as ng/L for serum TNFα and ng/mL protein for tissue markers. Results were analyzed using appropriate statistical methods, with values presented as mean ± standard deviation, and statistical significance set at $p < 0.05$.

Histological examination and validation of endometriosis lesions

Lesion tissue samples for the ELISA assay were obtained from the left peritoneum, while samples for histological examination were taken from the right peritoneum. Tissue samples were fixed in 10% neutral buffered formalin, processed, and embedded in paraffin blocks. Serial sections of 4 - 5 μm thickness were cut and stained with Hematoxylin and Eosin (H&E) using standard histological procedures. Hematoxylin stains cell nuclei dark blue or purple, while Eosin stains the cytoplasm and extracellular matrix in shades of pink to red, facilitating detailed observation of tissue anatomy and pathology.

For quantitative assessment, endometriosis lesion areas were measured using digital image analysis software (ImageJ, NIH, USA). High-resolution images of H&E-stained sections were captured at 100× magnification, and lesion boundaries were manually traced to calculate the total lesion area expressed in mm². The presence of endometrial glands lined with simple cuboidal epithelial cells and endometrial stroma were used as histological criteria for confirming endometriosis lesions.

The H&E-stained slides were independently analyzed by 2 experienced pathologists who were blinded to the treatment groups. Both pathologists evaluated the same histological features including gland morphology, stromal characteristics, and inflammatory infiltrate. Upon evaluation, no interobserver variability was observed in the histological interpretation, indicating consistency and reliability of the results.

Statistical analysis

All statistical analyses were performed using IBM SPSS Statistics version 28.0 (IBM Corp., Armonk, NY, USA). Data normality was assessed using the Shapiro-Wilk test due to the small sample size ($n < 50$). Based on the normality test results, parametric or non-parametric tests were selected accordingly.

The data on TNFα levels, BCL2, Caspase-3, and lesion area showed non-normal distribution and were analyzed using the non-parametric Kruskal-wallis test, followed by post-hoc Dunn's test with Bonferroni correction for multiple group comparisons. Ki-67 levels showed normal distribution and were analyzed using one-way ANOVA, followed by post-hoc Games-Howell test to assess differences between groups when equal variances were not assumed.

Data are presented as mean ± standard deviation (SD) for normally distributed variables and as median with interquartile range (IQR) for non-normally distributed variables. A p-value of <0.05 was considered statistically significant, and all tests were 2-tailed. The data on TNFα levels, BCL2, Caspase-3, and lesion area were analyzed using the non-parametric Kruskal-wallis test, followed by post-hoc Dunn's test for group comparisons. Meanwhile, the Ki-67 levels were analyzed using one-way ANOVA, followed by post hoc Games-Howell test to assess differences between groups. A p-value of <0.05 was considered statistically significant.

Results and discussion

Before discussing the therapeutic effects, this study conducted a phytochemical analysis of MBPE, which was used as the test substance. The purpose of this analysis was to identify bioactive compounds with potential pharmacological activities relevant to endometriosis pathology, particularly those associated with anti-inflammatory, antioxidant, and antiproliferative activities. Compound identification was carried out using LC-MS/MS-QTOF (Liquid Chromatography-Mass Spectrometry/Tandem Mass Spectrometry Quadrupole Time-of-Flight), a highly sensitive and accurate analytical method capable of detecting compounds at very low concentrations.

The analysis revealed that MBPE contains 9 flavonoid derivatives and 7 phenolic derivatives, both of which are known to play significant roles in inhibiting oxidative stress and inflammation. Among the identified flavonoids, licoflavone A and kaempferol were detected as major compounds, both recognized for their potent anti-inflammatory and antioxidant properties that are particularly relevant in managing endometrial inflammation and oxidative damage. Notable phenolic compounds included salidroside and coniferol, which have been extensively studied for their antiproliferative and anti-inflammatory effects against abnormal tissue growth. Among the identified compounds, licoflavone A showed the highest intensity, indicating it as the most abundant flavonoid in MBPE, followed by kaempferol and salidroside as the predominant phenolic compound. The presence of these bioactive compounds strengthens the scientific basis for utilizing MBPE as a potential therapeutic agent for the management of endometriosis. The details of the identified compounds are presented in **Table 1**.

Table 1 Identification of flavonoid and phenolic compounds in MBPE extract using LCMS/MS-QTOF analysis.

Compound name	PubChem id	Chemical formula	Observed RT (min)	Isotope match Mz RMS PPM	Isotope match Intensity RMS percent
Flavonoid					
Kaempferol	5280863	$C_{15}H_{10}O_6$	10.17	3.39	8.85
Licoflavone A	5319000	$C_{20}H_{18}O_4$	14.48	2.34	8.08
Maltol	8369	$C_6H_6O_3$	3.41	5.12	5.68

Compound name	PubChem id	Chemical formula	Observed RT (min)	Isotope match Mz RMS PPM	Isotope match Intensity RMS percent
Robinetin	5281692	$C_{15}H_{10}O_7$	9.24	2.66	2.66
Complanatuside	5492406	$C_{28}H_{32}O_{16}$	10.04	2.48	7.39
Genistein-7,4'-di-O-β-D-glucoside	91431845	$C_{27}H_{30}O_{15}$	9.79	2.23	8.00
Kaempferol 3-O-α-L-rhamnopyranosyl-(1 → 2)-β-D-glucopyranoside	5316673	$C_{21}H_{20}O_{10}$	9.38	3.56	9.50
Morin	5281670	$C_{15}H_{10}O_7$	12.75	3.34	7.94
Quercetin-3-O-β-D-gluco-pyranosyl(1 → 4)-α-L-rhamnopyranoside	5274585	$C_{21}H_{18}O_{13}$	8.86	1.42	3.83
Phenol					
4-Hydroxyacetophenone	7469	$C_8H_8O_2$	1.65	3.61	7.01
Coniferol	1549095	$C_{10}H_{12}O_3$	10.98	5.61	8.31
Dihydroeugenol	17739	$C_{10}H_{14}O_2$	7.73	3.96	7.77
L-Noradrenaline	439260	$C_8H_{11}NO_3$	3.59	3.80	7.00
2,4,5-Trihydeoxybenzaldehyde	643387	$C_7H_6O_4$	3.24	5.37	4.42
Salidroside	159278	$C_{14}H_{20}O_7$	11.53	4.38	5.12
Syringaldehyde	8655	$C_9H_{10}O_4$	9.86	5.39	8.34

Flavonoids are natural phytochemical compounds abundantly found in plants, fruits, and vegetables, and are well-known for their diverse biological activities, including anticancer, antioxidant, anti-inflammatory, and cardioprotective effects [23]. Certain flavonoids such as quercetin and kaempferol have been shown to effectively inhibit cell proliferation, promote apoptosis, and suppress the implantation and formation of ectopic lesions in endometriosis through the PI3K signaling pathway and regulation of PTEN and MMP9 gene expression [24,25]. Genistein has also been reported to increase the levels of antioxidant enzymes SOD and GPx in a rat model of endometriosis [26], while Licoflavone A exhibits anticancer properties by inhibiting VEGFR-2 and the PI3K/AKT-MEK/ERK pathways [27].

Beyond flavonoids, the broader category of phenolic compounds offers additional therapeutic opportunities, with phenolic derivatives demonstrating similarly promising bioactive properties. Coniferol and its derivatives, such as tripolinolate A, have demonstrated anti-inflammatory and anticancer properties [28]. 4-Hydroxyacetophenone has been shown to inhibit colon cancer metastasis through NM2C activation [29]. Salidroside exhibits neuroprotective and immunomodulatory effects via activation of the Nrf2/GPX4 and SIRT1 pathways, and is considered a potential therapeutic agent for psoriasis [30,31]. Syringaldehyde demonstrates significant potential as a multi-target compound with promising therapeutic activities, particularly for diabetes treatment, cardiovascular diseases, and inflammatory conditions through its interactions with multiple protein targets including TNF-α, IL-6, DPP-4, GLP-1R, and PPAR-γ, offering both antioxidant and anti-inflammatory mechanisms [32].

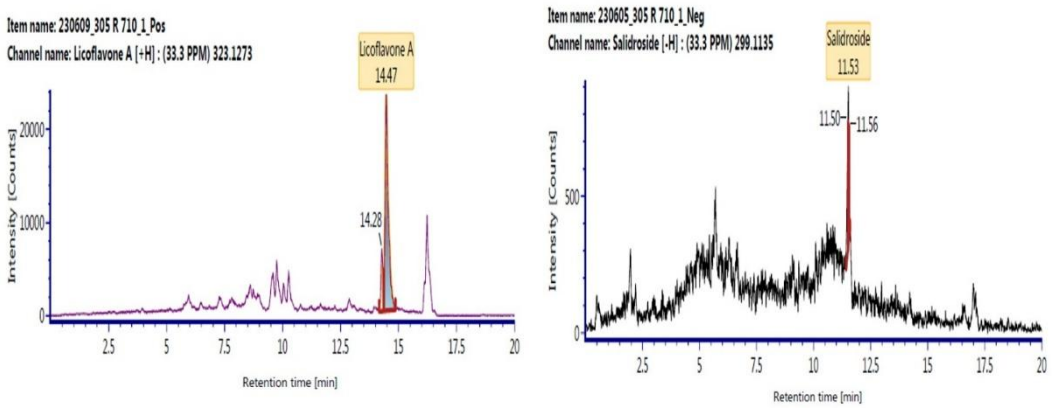

Figure 2 Chromatography of flavonoid and phenolic compounds.

Figure 2 shows the chromatogram of one of the flavonoid and phenolic compounds in MBPE. MBPE contains various compounds with different retention times, reflecting the diversity of chemical properties in the mixture. In the flavonoid chromatogram, the highest peak appears at a retention time of 14.47 min, identified as Licoflavone A, indicating that this compound is the dominant component with a signal intensity significantly higher than other peaks. Meanwhile, in the phenolic compound chromatogram, the dominant peak was detected at a retention time of 11.52 min, identified as salidroside, which also shows very high intensity compared to other phenolic compounds in the extract.

Table 2 Mineral content (ICP OES method) and vitamin content (HPLC-PDA Method) in MBPE.

Mineral and Vitamin	Unit	*Concentration*
Magnesium (Mg)	mg/100 g	4.74
Manganese (Mn)	mg/100 g	0.453
Zinc (Zn)	mg/100 g	0.29
Copper (Cu)	mg/100 g	0.17
Vitamin A (Retinol)	mg/100 g	0.1751
Vitamin E (Alpa Tokoferol)	mg/100 g	8.072

Minerals and vitamins are essential components in the human body that play important roles in maintaining health and supporting recovery processes from various medical conditions. As micronutrients, minerals such as calcium, magnesium, and zinc, as well as vitamins including A, C, D, and E, possess specific functions that can be directed to support particular therapies. These constituents not only act as metabolic enhancers but also function as enzymatic cofactors, antioxidants, and regulators of physiological functions. **Table 2** shows 4 minerals detected in the MBPE sample, while Selenium (Se) and Chromium (Cr) were not detected in the MBPE sample.

Molecular docking analysis of MBPE compounds targeting TNF-α receptor

Ligand structures were obtained from the PubChem database and modeled using Avogadro software. Geometry optimization was performed using the MMFF94 (Merck Molecular Force Field 94) method with 10,000 iterations to achieve the most stable minimum energy conformation. The crystal structure of the TNF Receptor (PDB ID: 1EXT) was obtained from the RCSB Protein Data Bank. Water molecules were removed to prevent interference during the docking process. Polar hydrogen atoms were added using Discovery Studio Visualizer (DSV) software due to their role in hydrogen bond formation between ligand-

receptor interactions [33]. Docking simulation was conducted using AutoDock Tools with a grid box configuration of 46×46×54 $Å^3$ positioned at the active binding site of the protein. The grid box dimensions were adjusted to ensure optimal flexibility in exploring ligand-receptor conformations without spatial constraints [34,35].

Table 3 Result in molecular docking of ligand to TNF receptor.

Ligand code	Ligand	Binding energy (kcal/mol)	Inhibition constant	Number of hydrogen bonds (HB)	Number of hydrophobic interaction (HI)
S01	Kaemferol	–6.62 kcal/mol	14.04 μM	6 HB: Glu131, Arg104, Cys98, Cys129	4 HI: Gln130, Cys98, Cys129
S02	Licoflavone A	–8.15 kcal/mol	1.06 μM	3 HB: Asn101, Arg104, Cys98	7 HI: Cys117, Cys129, Cys98
S03	Maltol	–4.25 kcal/mol	762.69 μM	1 HB: Arg104	1 HI: Cys98
S04	Robinetin	–6.53 kcal/mol	16.43 μM	3 HB: Asn101, Arg104, Cys98	2 HI: Cys129, Cys98
S05	Complanatuside	–6.27 kcal/mol	25.51 μM	5 HB: Arg104, Ser128, Cys98, Cys129, **Lys100**	5 HI: Cys117, Cys129, Cys98
S06	Genistein-7,4'-di-O-β-D-glucoside	–7.60 kcal/mol	2.70 μM	10 HB: Ser128, Thr135, Ser118, Gln102, Arg104, Cys98, Cys129	4 HI: **Lys100**, Cys117, Cys129
S07	Kaempferol 3-O-α-L-rhamnopyranosyl	–6.49 kcal/mol	17.36 μM	4 HB: **Lys100**, Arg104, Cys98	1 HI: Arg104
S08	Morin	–6.79 kcal/mol	10.57 μM	6 HB: Arg104, Glu131, Cys98, Cys129, **Lys100**	2 HI: Cys98
S09	Quercetin-3-O-β-D-glucopyranosyl	–6.53 kcal/mol	16.30 μM	5 HB: Asn101, Ser128, Ser118, **Lys100**	5 HI: Cys117, Cys129, Val125
S10	4-Hydroxyacetophenone	–4.91 kcal/mol	249.67 μM	3 HB: Gln102, Arg104, Cys98	2 HI: Cys98, Arg104
S11	Coniferol	–5.10 kcal/mol	182.24 μM	3 HB: **Lys100**, Arg104, Cys98	3 HI: Cys98, Arg104
S12	Dihydroeugenol	–5.11 kcal/mol	179.94 μM	3 HB: Arg104, Cys98	3 HI: Cys98, Arg104, Ile85
S13	L-Noradrenaline	–5.25 kcal/mol	142.68 μM	6 HB: Arg104, Glu131, Cys98, Gln102, Gln130	1 HI: Cys98

Ligand code	Ligand	Binding energy (kcal/mol)	Inhibition constant	Number of hydrogen bonds (HB)	Number of hydrophobic interaction (HI)
S14	2,4,5-Trihydeoxybenzaldehyde	–4.82 kcal/mol	294.18 µM	5 HB: Arg104, Glu131, Cys98, **Arg99**	2 HI: Cys98, Arg104
S15	Salidroside	–5.91 kcal/mol	46.90 µM	4 HB: Gln131, Asn101, Cys98	3 HI: Cys117, Cys129, Cys98
S16	Syringaldehyde	–4.62 kcal/mol	408.00 µM	3 HB: Arg104, Cys98	4 HI: Arg104, Cys98, Ile85
S17	Vitamin A (Retinol)	–7.73 kcal/mol	2.16 µM	1 HB: Thr135	3 HI: Cys117, Cys129, Cys98
S18	Vitamin E (Alpa Tokoferol)	–7.84 kcal/mol	1.78 µM	2 HB: Thr135, Ser118	4 HI: Cys117, Cys129, Cys98, Ile85
TNF-α	TNF-α	–7.05 kcal/mol	6.74 µM	3 HB: **Lys100**, Arg104, Cys98	3 HI: Cys98, Arg104

The molecular docking results of ligands with TNF receptors show the binding energy and inhibition constant of each ligand compared to TNF-α as the reference ligand. Ligands S02 and S18 demonstrated the lowest binding energies of –8.15 and –7.84 kcal/mol, respectively, with inhibition constants of 1.06 and 1.78 µM, which were lower compared to TNF-α (–7.05 kcal/mol; 6.74 µM). This indicates that both ligands possess a stronger binding affinity to the TNF receptor compared to the reference ligand. Conversely, ligands such as S03 and S16 showed relatively high binding energies of –4.25 and –4.62 kcal/mol, respectively, with inhibition constants of 762.69 and 408.00 µM, reflecting lower binding affinity. Overall, the variation in binding energy and inhibition constant of each ligand provides insights into different binding potentials, where several ligands demonstrated superior performance compared to TNF-α as the reference. This suggests that the test ligands have a significantly higher potential to serve as active compounds that could be developed as drug candidates. Exhibiting negative binding energy values indicates that ligands can interact with the target using minimal energy for the interaction, while low binding free energy values demonstrate stable ligand-target complexes [36].

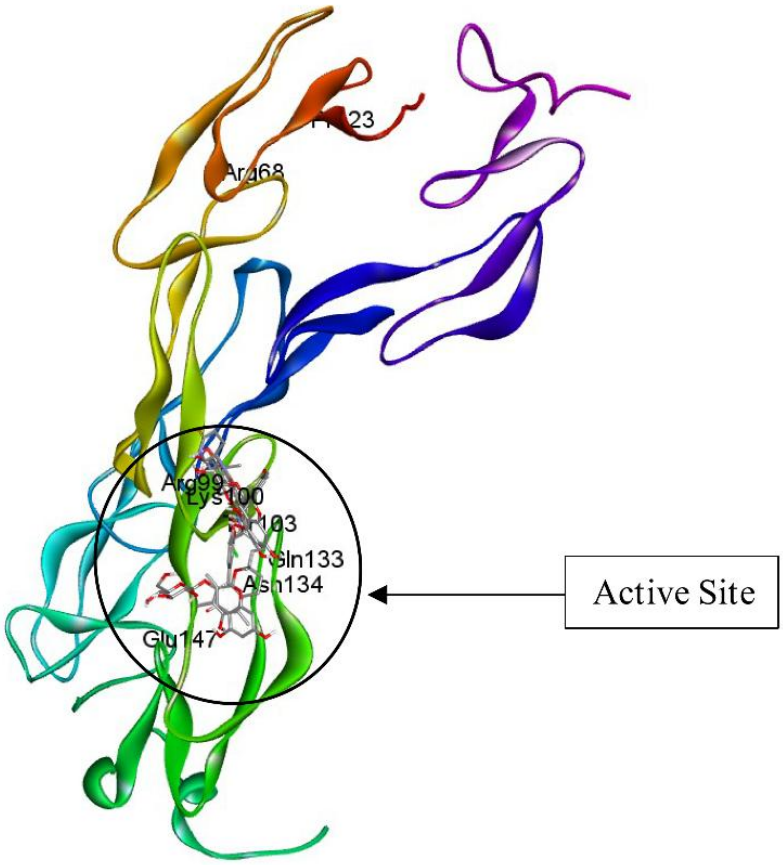

Figure 3 Molecular docking visualization of the TNF receptor active site.

The ligands were detected at the active site of the TNF receptor with interactions involving key residues, particularly Lys100 and Arg99, which frequently appeared as dominant residues in binding. Lys100 and Arg99 are known to form strong electrostatic interactions, thereby contributing significantly to the stability of the ligand-receptor complex. Additionally, other residues such as Tyr103, Gln134, and Glu147 were also identified to establish additional interactions, including hydrogen bonds and hydrophobic interactions, which support ligand binding at the active site. The presence of Lys100 and Arg99 as the most frequently involved residues indicates that both serve as primary interaction centers in the binding mechanism at the TNF receptor, reinforcing the relevance of these residues in designing ligands with high affinity.

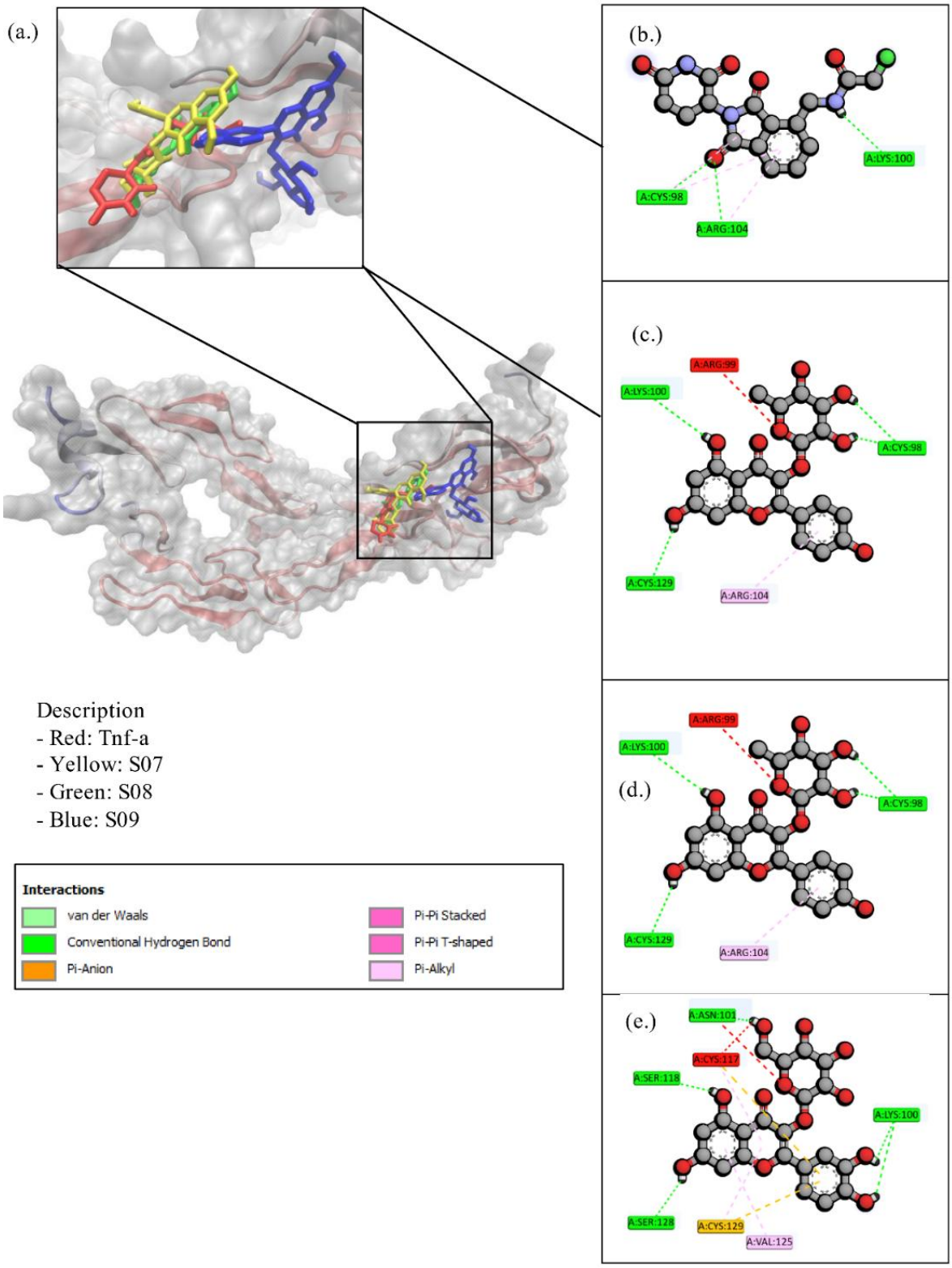

Figure 4 Molecular docking visualization of ligand-protein interactions (a) TNF receptor (b) TNF-α (c) Kaempferol 3-O-α-L-rhamnopyranoside (d) Morin (e) Quercetin-3-O-β-D-glucopyranoside.

Visualization was performed using DSV and VMD software to examine the interaction between ligands and targets by assessing conformational compatibility. The conformational compatibility of test ligands was compared with native ligands to confirm binding free energy values, as active ligands must bind to specific amino acid residues at the binding site to produce inhibition or induction of activity. The molecular

interactions of ligands with TNF receptors have been analyzed, where ligands S07, S08, S09, and TNF-α demonstrated the involvement of important residues such as Lys100 and Arg99. For ligand S07, 4 hydrogen bonds (HB) were formed involving Lys100, Arg104, and Cys98, along with 1 hydrophobic interaction (HI) at Arg104. Ligand S08 generated 6 HB with residues including Lys100, Arg104, and Cys98, as well as 2 HI at Cys98. Ligand S09 showed 5 HB, including Lys100, and 5 HI involving residues such as Cys129 and Val125. As a comparison, TNF-α formed 3 HB with Lys100, Arg104, and Cys98, along with 3 HI at residues Cys98 and Arg104. These results indicate that ligands S08 and S09 possess more diverse interactions compared to TNF-α, particularly in the number of HB and HI. The frequent appearance of Lys100 and Arg99 as primary interaction centers confirms the important role of these residues in supporting ligand-receptor complex stability, with S08 showing promising potential based on the number and quality of its interactions.

These molecular docking findings provide significant insights for anti-inflammatory drug development, particularly for TNF-α-mediated diseases including endometriosis, rheumatoid arthritis, and inflammatory bowel disease. Compounds S02 (Licoflavone A) and S18 (Vitamin E) demonstrated superior binding affinity (Ki = 1.06 and 1.78 μM, respectively) compared to endogenous TNF-α (Ki = 6.74 μM), indicating potential as competitive TNF receptor antagonists. The strong interactions with key residues Lys100 and Arg99 suggest these compounds can effectively block TNF-α signaling pathways. In endometriosis, where TNF-α drives ectopic tissue proliferation and chronic pain, these compounds may inhibit downstream NF-κB activation, reducing pro-inflammatory cytokine production (IL-1β, IL-6) and disease progression. The favorable safety profile of natural flavonoids and vitamin E supports their development as alternatives or adjuvants to current synthetic TNF-α inhibitors, offering potential therapeutic advantages with reduced adverse effects.

The effects of MBPE on TNFα, Ki-67, BCL2, and Caspase 3 expression

The data in **Table 1** indicate that the administration of MBPE treatment began on day 15 following the establishment of the endometriosis model, which corresponds to day 45 after the initial surgery. Before analyzing the therapeutic effects of the MBPE, normality and homogeneity tests were conducted to determine the appropriate statistical analysis method.

Table 4 Results of TNFα, Ki-67, BCL2, and Caspase 3 level analysis.

Variable	Group						*p*-value
	NC	NGC	DLBS1442	MBPE200	MBFE300	MBPE400	
	Mean						
TNFα: Day 31	155.27	171.61	173.69	174.15	172.21	166.29	
SD	34.87	42.09	31.25	42.33	32.61	35.17	
Shapiro Wilk	0.944*	0.020	0.517*	0.157*	0.859*	0.604*	
Kruskal-Wallis							0.848
TNFα: Day 45	147.21	182.15	137.56	153.85	145.74	131.94	
SD	39.11	23.81	29.65	37.56	22.62	24.86	
Shapiro Wilk	0.292*	0.612*	0.601*	0.028	0.646*	0.596*	
Kruskal-Wallis							0.024***
Ki-67	4.130	4.909	3.884	4.101	4.306	3.841	
SD	0.099	0.308	0.458	1.064	0.394	0.286	
Shapiro Wilk	0.981*	0.749*	0.124*	0.801*	0.071*	0.617*	
Levene Test							0.001
One Way Anova							0.003***

Variable	Group						*p*-value
	NC	NGC	DLBS1442	MBPE200	MBFE300	MBPE400	
	Mean						
BCL2	6.423	5.234	8.250	7.318	7.597	8.556	
SD	0.785	1.552	1.762	2.095	1.393	2.773	
Shapiro Wilk	0.382*	0.181*	0.824*	0.966*	0.811*	0.016	
Kruskal-Wallis							0.004***
Caspase 3	1.580	1.044	1.373	1.280	1.250	1.511	
SD	0.180	0.175	0.253	0.311	0.328	0.318	
Shapiro Wilk	0.122*	0.001	0.076*	0.493*	0.833*	0.027	
Kruskal-Wallis							0.001***

TNFα levels were measured at 2 time points to assess the temporal progression of inflammatory response: Day 31 (before treatment initiation) and day 45 (after 14 days of treatment). At day 31 (baseline), the Shapiro-Wilk test showed normal distribution in most groups except NGC (p = 0.020), requiring Kruskal-wallis analysis. No significant differences were observed among groups (p = 0.848), with all groups showing elevated inflammatory levels: NC (155.27 ± 34.87), NGC (171.61 ± 42.09), DLBS1442 (173.69 ± 31.25), MBPE200 (174.15 ± 42.33), MBPE300 (172.21 ± 32.61), and MBPE400 (166.29 ± 35.17). At day 45 (post-treatment), significant differences emerged among groups (p = 0.024), with only MBPE200 showing non-normal distribution (p = 0.028). The NGC group demonstrated increased TNFα levels (182.15 ± 23.81), while treatment groups showed reductions, with MBPE400 (131.94 ± 24.86) and DLBS1442 (137.56 ± 29.65) exhibiting the most significant decreases.

Ki-67 was analyzed using one-way ANOVA after confirming normal distribution across all groups, although Levene's test indicated non-homogeneous variances (p = 0.001). Results showed significant differences among groups (p = 0.003). The NGC group demonstrated the highest Ki-67 expression (4.909 ± 0.308), while MBPE400 (3.841 ± 0.286) and DLBS1442 (3.884 ± 0.458) showed the lowest levels, even below the normal control NC (4.130 ± 0.099).

BCL2 was analyzed using the Kruskal-Wallis test as the MBPE400 group did not follow normal distribution (Shapiro-Wilk p = 0.016). Results showed significant differences among groups (p = 0.004). The pathological control NGC showed the lowest BCL2 levels (5.234 ± 1.552), while treatment groups demonstrated increases: MBPE400 (8.556 ± 2.773), DLBS1442 (8.250 ± 1.762), MBPE300 (7.597 ± 1.393), and MBPE200 (7.318 ± 2.095).

Caspase-3 was analyzed using the Kruskal-Wallis test due to non-normal distribution in NGC (p = 0.001) and MBPE400 (p = 0.027) groups. Results showed significant differences among groups (p = 0.001). The NGC group exhibited the lowest Caspase-3 activity (1.044 ± 0.175), while MBPE400 (1.511 ± 0.318) demonstrated the greatest recovery of activity, most closely approaching the normal control NC (1.580 ± 0.180).

Further statistical analyses were conducted based on data normality and homogeneity assessments. The Ki-67 variable was analyzed using one-way ANOVA followed by the Games-Howell post-hoc test, which is specifically designed to handle unequal variances among groups. TNFα, BCL2, and Caspase-3 variables were analyzed using the Kruskal-Wallis test followed by Dunn's post-hoc test due to non-normal data distributions, with variance homogeneity testing being irrelevant for non-parametric analyses. The post-hoc test results are presented in **Figure 3**.

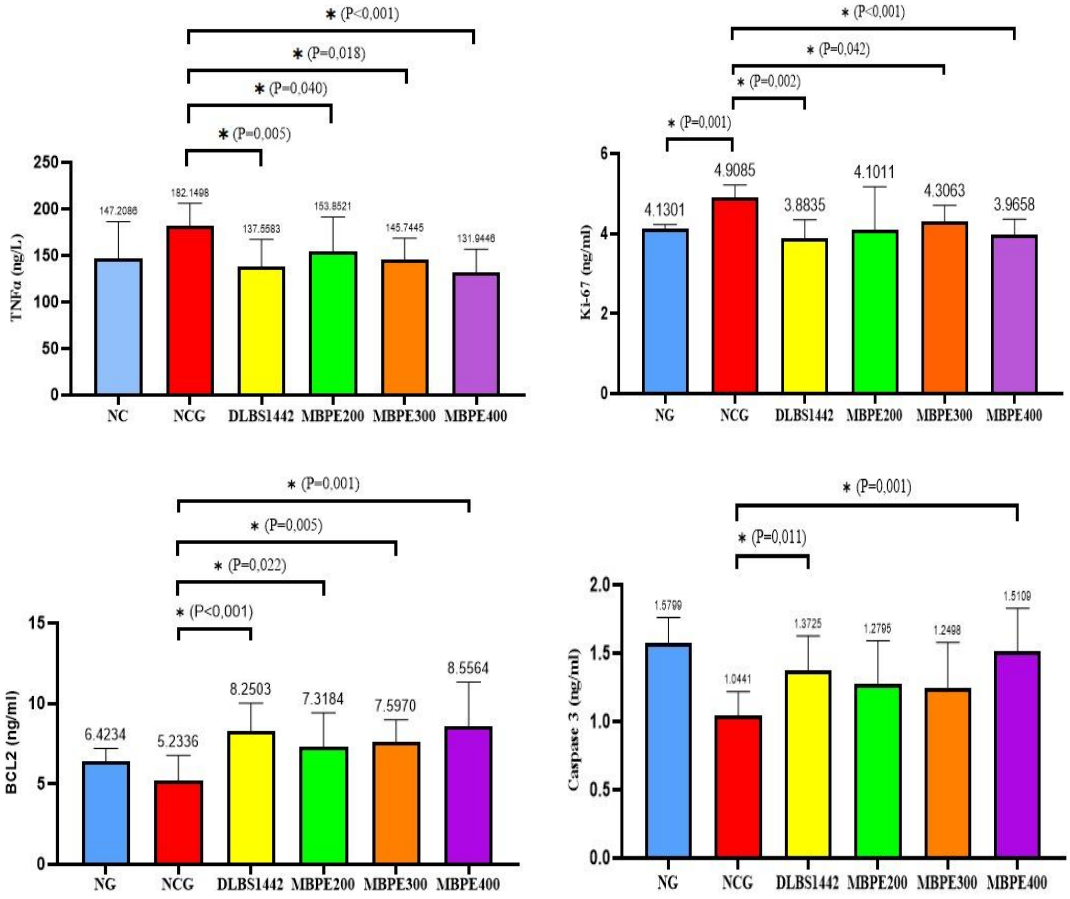

Figure 5 Comparison of TNFα, Ki-67, BCL2, and Caspase-3 levels among treatment groups. Statistical analysis was performed using ANOVA Games-Howell and Kruskal-Wallis Dunn tests. A p-value <0.05 was considered statistically significant.

The Post Hoc Dunn test results for TNF-α levels revealed significant differences between the negative control group (NCG) and all treatment groups, namely the DLBS1442 group (p = 0.005), MBPE200 (p = 0.040), MBPE300 (p = 0.018), and MBPE400 (p < 0.001). These findings indicate that MBPE administration was able to reduce TNF-α levels in the endometriosis rat model, with the MBPE400 dose demonstrating the most significant effect. Similar analysis of Ki-67 levels using the Post Hoc Games-Howell test showed significant differences between the NCG group and all other groups, including NG, DLBS1442, MBPE300, and MBPE400 with p-values <0.05. These results confirm that MBPE intervention was effective in reducing Ki-67 levels in the endometriosis model, with MBPE400 as the most effective dose. Evaluation of BCL2 levels through the Post Hoc Dunn test demonstrated significant differences between the NCG group compared to the DLBS1442 group (p < 0.001), MBPE200 (p = 0.022), MBPE300 (p = 0.005), and MBPE400 (p = 0.001). These data illustrate that both MBPE intervention and standard DLBS1442 treatment provided a substantial impact on increasing BCL2 levels relative to the negative control group. Meanwhile, Caspase 3 level testing using the Post Hoc Dunn method revealed significant differences between the NCG group versus the DLBS1442 group (p = 0.011) and the MBPE400 group (p = 0.001). These results confirm that MBPE intervention was effective in increasing Caspase 3 levels in the endometriosis model, with MBPE400 as the most effective dose.

Interestingly, no significant differences were found between treatment groups, either between the DLBS1442 group and MBPE groups (200, 300, 400), or among the various MBPE doses themselves. Overall, the findings of this study confirm that all administered treatments successfully reduced TNF-α and Ki-67 levels and increased BCL2 and Caspase 3 levels compared to

the negative control group. However, no single treatment demonstrated striking superiority over other treatments, suggesting that all interventions possess relatively comparable levels of effectiveness in addressing the investigated endometriosis parameters.

This study demonstrates that the administration of MBPE significantly improves inflammatory conditions, cell proliferation, and apoptosis in a rat model of endometriosis. Interventions with 3 dosages (200, 300, and 400 mg/kg body weight) yielded promising results, especially in the MBPE400 group, which approached or matched the effects of the standard therapy (DLBS1442) in several parameters.

Analysis of TNF-α levels showed significant reductions across all treatment groups (MBPE200, MBPE300, MBPE400), with the greatest decrease observed in the MBPE400 group (131.84 pg/mL). This effect is likely related to the activity of flavonoid compounds such as kaempferol and genistein, which act via inhibition of the NF-κB pathway. Qu *et al*. [37] demonstrated that kaempferol significantly reduces serum levels of pro-inflammatory cytokines including TNF-α, IL-1β, and IL-6 by suppressing the LPS-TLR4-NF-κB signaling pathway. The study showed that kaempferol pretreatment inhibited DSS-induced expression of TLR4, MyD88, p-NF-κB-P65, and NLRP3, thereby downregulating transcription of inflammatory signaling molecules while increasing IL-10 mRNA expression. Genistein has also been reported to reduce TNF-α and IL-6 expression and modulate estrogen receptor expression in a rat endometriosis model [38]. These findings are consistent with Savitri *et al*. [39], who demonstrated that MBPE exhibits anti-inflammatory effects in acne vulgaris by suppressing nodule formation, inhibiting bacterial growth, and reducing proinflammatory cytokines such as IL-1α, IFN-γ, TNF-α, and IL-8.

Furthermore, TNFα is known to play a dual role in the regulation of apoptosis, particularly via the extrinsic pathway involving activation of TNFR1 and the DISC complex, which subsequently activates Caspase-8 and Caspase-3 as executors of apoptosis. Therefore, the reduction of TNFα levels in the MBPE groups may reflect a more balanced modulation of apoptotic signaling. This aligns with the study by Zabala *et al*. [40], which demonstrated that the regulation of TNFα is directly related to Caspase-3 activation through programmed cell death pathways.

A significant decrease in Ki-67 levels, a marker of cell proliferation, was observed in the MBPE groups, especially at the 400 mg/kg body weight dosage. This effect is likely attributed to bioactive compounds such as genistein and licoflavone A. Genistein has been reported to arrest the cell cycle at the G2/M phase and reduce the expression of proliferative proteins such as Skp2 [41]. Meanwhile, licoflavone A was reported by Hongxia *et al.* [27] to inhibit cancer cell proliferation through suppression of Cyclin D1 and c-Myc expression, as well as modulation of the VEGFR-2/PI3K/AKT/MEK/ERK signaling pathway. Additionally, quercetin, also present in MBPE, exhibits therapeutic effects by enhancing decidualization and inhibiting the AKT/ERK1/2 pathways while activating p53. The findings of Delenko *et al*. [42] support these observations, noting that quercetin can induce apoptosis in endometrial cells resembling a senescent phenotype.

Theoretically, a decrease in BCL2 levels is expected to indicate apoptosis activation since BCL2 functions as an anti-apoptotic protein. However, this study observed an increase in BCL2 levels, particularly in the MBPE400 group. This phenomenon may be explained by the hypothesis of an adaptive or compensatory response to biological stress induced by the extract administration. In the context of endometriosis, the inflammatory microenvironment and short-term exposure to bioactive compounds can trigger a transient increase in BCL2 as a cellular defense mechanism against stress or apoptotic signals that have not yet become dominant.

Several studies support that BCL2 levels do not always correlate linearly with cell death. Research by Chimento *et al*. [43] demonstrated that polyphenolic compounds can induce a transient increase in BCL2 before Caspase-3 activation. Similarly, Delenko *et al*. [42] reported that phytochemicals may trigger senescence pathways before apoptosis occurs. Therefore, elevated BCL2 expression does not necessarily indicate apoptosis resistance but may represent part of a transient molecular dynamic before full activation of the cell death pathway.

The significant increase in Caspase-3 levels observed in the MBPE groups, particularly at the 400 mg/kg dose, indicates that apoptosis pathways remain

actively engaged as a mechanism for cell elimination. Caspase-3 is known as the primary executioner enzyme in apoptosis, and its elevation reflects successful intervention in promoting the death of ectopic endometrial cells. This apoptotic activation is likely supported by bioactive compounds such as genistein, morin, and licoflavone A, each reported inducing apoptosis through various mechanisms, including p53 activation, disruption of mitochondrial integrity, and inhibition of the PI3K/AKT pathway [27,41,44]. These findings align with Barroso *et al.* [45], who showed that green banana peel extract (Musa cavendish) (MHE) exerts significant cytotoxic effects on several cancer cell lines (HepG2, A-375, MCF-7, and Caco-2) via apoptosis and necrosis mechanisms. The antiproliferative effects of MHE were further supported by mitochondrial membrane depolarization and dose-dependent increases in reactive oxygen species (ROS), suggesting similar mechanisms may occur in ectopic endometrial cells.

Molecular docking results demonstrated a clear correlation with the biomarker changes observed in *in vivo* assays. The high binding affinity of compounds S02 ($\Delta G = -8.2$ kcal/mol) and S18 ($\Delta G = -7.8$ kcal/mol) toward TNF receptor provided molecular explanation for the significant reduction in TNF-α pathway activity observed *in vivo*. This TNF receptor inhibition blocked the binding site for endogenous TNF-α, thereby preventing downstream signaling activation which subsequently affected other biomarkers: Decreased Ki-67 levels indicating reduced cell proliferation, increased Caspase-3 activity levels demonstrating apoptosis induction in ectopic endometrial cells, and BCL2 level modulation reflecting apoptosis pathway regulation. Molecular interactions through hydrogen bonds with Lys100 residue and hydrophobic interactions with Arg99 on the TNF receptor binding domain constitute the molecular basis of the anti-inflammatory and anti-proliferative activities observed in experimental animal models.

Interestingly, the concurrent elevation of BCL2 levels and Caspase-3 activation demonstrates active apoptotic processes amid complex molecular and cellular dynamics. This phenomenon reflects the transition from survival to cell elimination phases and underscores the necessity for future investigations employing real-time protein analysis or Bax/BCL2 ratio assessments as supplementary parameters. Within the pathophysiological context of endometriosis, this apoptotic modulation assumes particular significance, as aberrant cell survival and apoptosis resistance contribute to ectopic endometrial proliferation and lesion persistence [46]. The observed Caspase-3 activation indicates that MBPE treatment effectively promotes programmed cell death in endometriotic lesions, whereas elevated BCL2 levels may represent compensatory cellular responses during therapeutic intervention [42]. The bioactive compounds in MBPE, particularly genistein and quercetin, presumably modulate these apoptotic pathways through established effects on mitochondrial membrane potential and death receptor signaling cascades. This bidirectional regulation of pro- and anti-apoptotic markers suggests that MBPE exerts therapeutic efficacy by restoring the homeostatic balance between cell survival and death, consequently inducing lesion regression—a pivotal mechanism underlying endometriosis treatment success, consistent with Silva-Pinto *et al.* [47] findings on the multifaceted therapeutic roles of flavonoids through multiple cellular pathway modulation.

In this study, the MBPE400 group demonstrated performance comparable to the standard therapy group (DLBS1442) in several parameters, including reduced TNFα levels and increased Caspase-3 levels. DLBS1442, containing Phaleria macrocarpa extract, is a widely sed herbal therapy in Indonesia for endometriosis treatment. These findings suggest that MBPE exhibits relevant anti-inflammatory and pro-apoptotic effects, supported by a bioactive compound profile that promotes multi-mechanistic activity. This indicates that MBPE has the potential for development as an alternative or complementary phytochemical-based therapy for endometriosis management.

Effects of MBPE therapy on endometriosis lesions

The size of endometriosis lesions is an important indicator in assessing the effectiveness of therapy in inhibiting the development and spread of these lesions. The size of the endometriosis lesions is presented in **Figure 4**.

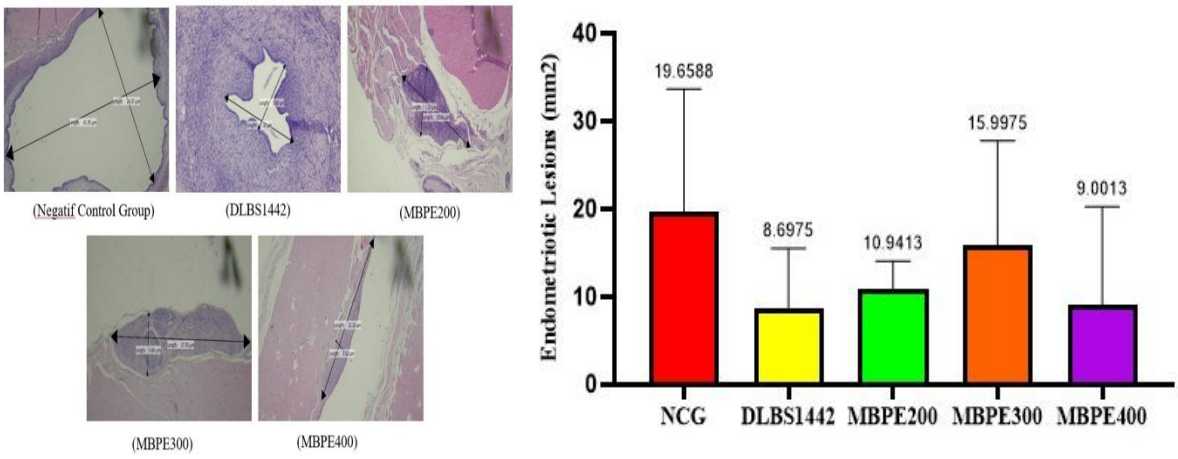

(A) (B)

Figure 6 Histopathological analysis of the effect of MBPE on endometriosis lesion area in a rat model of endometriosis. (A) H&E staining of endometriosis lesions (mm²) showing varying lesion sizes. (B) Bar chart illustrating the comparative differences in the mean values of endometriosis lesion area (mm²). Statistically significant at $p < 0.001$ based on the Kruskal Wallis test.

The measurement of the endometriosis lesion area in this study was conducted using the Hematoxylin-Eosin (HE) staining method, which enables accurate histological identification of tissue morphology. The visual analysis results presented in **Figure 6(A)** demonstrate striking differences in lesion area between the negative control group (NCG) compared to the intervention groups, namely the DLBS1442 group and all MBPE groups (200, 300, 400). This visual comparison illustrates that both MBPE administration and standard DLBS1442 therapy provided substantial impact in reducing endometriosis lesion size relative to the negative control group. These visual findings were confirmed through Kruskal-Wallis statistical analysis, the results of which are presented in **Figure 6(B)**. The statistical test results showed that all treatment groups, both MBPE and standard DLBS1442 therapy, experienced a significant reduction in lesion area compared to the negative control group (NCG). Specifically, the most significant lesion area reduction occurred in the standard DLBS1442 therapy group, followed by the MBPE400 group as the dose demonstrating the highest effectiveness among the extract groups.

The observed reduction in the size or area of endometriotic lesions in the treatment groups suggests that MBPE administration effectively inhibits the growth and invasion of ectopic endometrial tissue—one of the key characteristics in the pathogenesis of endometriosis. This effect is presumed to result from the synergistic activity of various bioactive compounds within MBPE, such as genistein, quercetin, and kaempferol, which are known for their anti-inflammatory, antiproliferative, and pro-apoptotic properties.

Several previous studies have supported this mechanism. Sutrisno *et al.* [38] reported that oral administration of genistein for 14 days in a rat model of endometriosis significantly reduced the volume and diameter of the implants, as well as decreased the expression of estrogen receptors and VEGF, which are associated with lesion growth.

Flavonoids genistein, quercetin, and kaempferol demonstrate promising therapeutic potential in reducing endometriotic lesions through complementary and distinct mechanisms of action. Genistein functions as an anti-inflammatory and immunomodulatory agent by inhibiting the expression of pro-inflammatory cytokines, including nuclear factor-κB (NF-κB), estrogen receptor beta (ESR2), cyclooxygenase-2 (COX-2), and prostaglandin E (PGE), with an effective dose of 54 mg daily proven as an alternative treatment for endometrial hyperplasia in premenopausal women [48]. Quercetin provides a unique therapeutic approach through senolytic activity that selectively eliminates senescent cells by inhibiting AKT-ERK1/2 signaling pathways and activating p53 to induce specific apoptosis, while simultaneously enhancing endometrial

decidualization through upregulation of biomarkers IGFBP1 and PRL, which are crucial for restoring reproductive function and reducing endometriosis-associated infertility [42]. Meanwhile, kaempferol exhibits multi-target mechanisms through modulation of the PI3K/PTEN/MMP9 pathway to reduce cellular migration and invasion, and operates via interactions with nuclear receptors (PPARγ, PPARα, NR4A1) that regulate inflammation, angiogenesis, and apoptosis, including inhibition of oncogenic pathways such as EGFR, c-Myc, and mTOR [25,49].

In addition to these specific mechanisms, research by Wulandari *et al.* [13] demonstrated that flavonoids in Phyllanthus niruri effectively reduced levels of IL-1β, MDA, and MMP-9, and significantly decreased the area of endometriotic lesions. These findings reinforce the role of the anti-inflammatory and antioxidant properties of flavonoids in suppressing lesion progression at the histopathological level. Consistent with these findings, Situmorang *et al.* [50] reported that flavonoids in Sulawesi propolis extract were capable of inhibiting the growth of endometriotic tissue in a rat model by enhancing apoptotic activity and reducing inflammation. Collectively, these studies support the notion that flavonoid compounds, including those found in MBPE, possess significant therapeutic potential in treating endometriosis through multimodal mechanisms.

Moreover, this finding is further supported by the biomarker data in this study, which showed a decrease in TNF-α and Ki-67 levels and an increase in Caspase-3 levels. These biomarker changes collectively indicate a suppression of inflammation and proliferation, alongside the stimulation of apoptosis. The combination of these mechanisms likely contributes to the regression of lesion size observed through HE staining.

Although the most substantial reduction in lesion area was achieved by the DLBS1442 group, the MBPE400 group demonstrated a competitive level of effectiveness. This indicates that MBPE holds considerable potential as a natural-based alternative therapy candidate, especially with further development in dosage optimization, formulation, or active compound fractionation.

Nevertheless, this study has several limitations that warrant consideration. The MBPE utilized was a crude extract without isolation of its active compounds; therefore, the specific efficacy of individual components remains unclear. Although ELISA analysis provided quantitative information regarding inflammatory, proliferation, and apoptotic parameters, protein-level and gene expression analyses such as Western blot and qPCR would yield deeper insights into the underlying molecular mechanisms. Evaluation of specific signaling pathway modulation, particularly the NF-κB and PI3K/AKT pathways, through these molecular techniques would strengthen the interpretation of MBPE's mechanism of action and will constitute the focus of future investigations. Furthermore, the utilization of an animal model limits the generalizability of these findings to human subjects, and the long-term safety profile and potential adverse effects of MBPE administration remain to be comprehensively evaluated.

Conclusions

In conclusion, the administration of MBPE at a dose of 400 mg/kg body weight demonstrated significant efficacy in improving various parameters related to endometriosis, including a reduction in TNF-α levels (inflammation), inhibition of cell proliferation (Ki-67), increased regulation of apoptosis (Caspase 3), and reduction in endometriotic lesion size. Compared to standard therapy, MBPE showed superior performance, particularly in reducing inflammatory markers (TNF-α levels) and regulating apoptosis (Caspase 3 levels). Furthermore, MBPE demonstrated comparable effectiveness in controlling cell proliferation and reducing lesion size. These findings suggest that MBPE offers promising therapeutic potential compared to conventional treatment modalities for certain key parameters.

However, further investigation is needed to validate these preliminary results. Future research should focus on the isolation and characterization of individual bioactive compounds within MBPE, dose optimization through comprehensive dose-response studies, development of more effective therapeutic formulations, clinical trials in humans, and long-term mechanistic studies. A comprehensive evaluation of the long-term safety profile is also a crucial prerequisite before clinical translation can occur. The limitations of this study, including the use of animal models and the relatively short treatment duration, should be considered

when interpreting the results and designing future research plans.

Acknowledgments

The authors would like to express their sincere gratitude to the Integrated Research and Testing Laboratory and the Anatomical Pathology Laboratory, at Gadjah Mada University, Indonesia, for their valuable support and assistance throughout this study.

Declaration of Generative AI in Scientific Writing

In the preparation of this manuscript, the authors utilised generative artificial intelligence tools specifically ChatGPT (OpenAI, version GPT-4) and Claude (Anthropic, version Claude 3) strictly for the purpose of language enhancement, including editing and grammatical checks. We hereby explicitly affirm that these tools were not employed in any capacity for generating scholarly content, formulating ideas, analysing data, interpreting results, or drawing conclusions. The authors assume full and sole responsibility for the entire intellectual content, accuracy, and integrity of this published work.

CRediT Author Statement

Siti Maesaroh: Conceptualization, Methodology, Formal analysis, Resources, Investigation, Validation, Project administration, and writing-original draft.

Soetrisno: Project administration, Data curation, Formal analysis, Investigation

Harijono Kario Sentono: Data curation, Formal analysis, Investigation

Dono Indarto: Methodology, Data curation, Formal analysis, Investigation, and writing-original draft.

References

[1] A Bala, MA Moga, L Dima, CG Dinu, CC Martinescu, DE Panait, CA Irimie and CV Anastasiu. An overview on the conservative management of endometriosis from a naturopathic perspective: Phytochemicals and medicinal plants. *Plants* 2021; **10(3)**, 587.

[2] X Cai, M Liu, B Zhang, SJ Zhao and SW Jiang. Phytoestrogens for the management of endometriosis: Findings and issues. *Pharmaceuticals* 2021; **14(6)**, 569.

[3] K Zondervan, CM Becker and SA Missmer. Endometriosis. *The New England Journal of Medicine* 2020; **382(13)**, 1244-1256.

[4] R Kapoor, CA Stratopoulou and MM Dolmans. Pathogenesis of endometriosis: New insights into prospective therapies. *International Journal of Molecular Sciences* 2021; **22(21)**, 11700.

[5] LDGC Riccio, P Santulli, L Marcellin, MS Abrão, F Batteux and C Chapron. Immunology of endometriosis. *Best Practice and Research: Clinical Obstetrics and Gynaecology* 2018; **50**, 39-49.

[6] T Zhang, CD Carolis, GCW Man and CC Chiu. The link between immunity , autoimmunity and endometriosis: A literature update. *Autoimmunity Reviews* 2018; **17(10)**, 945-955.

[7] J Wu, H Xie, S Yao and Y Liang. Macrophage and nerve interaction in endometriosis. *Journal of Neuroinflammation* 2017; **14(1)**, 53.

[8] BG Patel, EE Lenk, DI Lebovic, Y Shu, J Yu and RN Taylor. Pathogenesis of endometriosis: Interaction between Endocrine and inflammatory pathways. *Best Practice and Research: Clinical Obstetrics and Gynaecology* 2018; **50**, 50-60.

[9] E Piriyev, M Mariella, S Schiermeier and R Thomas. Significance of Ki67 expression in endometriosis for infertility. *European Journal of Obstetrics and Gynecology and Reproductive Biology* 2022; **272**, 73-76.

[10] YJ Cho, SH Lee, JW Park, M Han, MJ Park and SJ Han. Dysfunctional signaling underlying endometriosis: Current state of knowledge. *Journal of Molecular Endocrinology* 2018; **60(3)**, R97-R113.

[11] C Kaya, I Alay, H Guraslan, A Gedikbasi, M Ekin, SE Kaya, E Oral and L Yasar. The role of serum caspase 3 levels in prediction of endometriosis severity. *Gynecologic and Obstetric Investigation* 2018; **83(6)**, 576-585.

[12] HS Taylor, LC Giudice, BA Lessey, MS Abrao, J Kotarski, DF Archer, MP Diamond, E Surrey, NP Johnson, NB Watts, JC Gallagher, JA Simon, BR Carr, WP Dmowski, N Leyland, JP Rowan, WR Duan, J Ng, B Schwefel, JW Thomas, …, K Chwalisz. Treatment of endometriosis-associated pain with elagolix, an oral GnRH antagonist. *New England Journal of Medicine* 2017; **377(1)**, 28-40.

[13] ET Wulandari, S Soetrisno, B Purwanto, R Reviono, B Wasita and A Laqif. Impacts of *Phyllanthus niruri* extract on biomarker levels, macrophage count, and lesion area in an endometriotic rat model. *Narra J* 2024; **4(3)**, e1002.

[14] J Song, J Ham, S Park, SJ Park, HS Kim, G Song and W Lim. Alpinumisoflavone activates disruption of calcium homeostasis, mitochondria and autophagosome to suppress development of endometriosis. *Antioxidants* 2023; **12(7)**, 1324.

[15] LY Zhang, TT Huang, LP Li, DP Liu, Y Luo, W Lu, N Huang, PP Ma, YQ Liu, P Zhang and BC Yang. ITRAQ-based proteomics analysis of human ectopic endometrial stromal cells treated by Maqian essential oil. *BMC Complementary Medicine and Therapies* 2023; **23(1)**, 427.

[16] PAR Yulis and Y Sari. Aktivitas antioksidan dari limbah kulit pisang muli (*Musa acuminata* Linn) dan kulit pisang kepok (*Musa paradisiaca formatypica*) (*in Indonesian*). *Al-Kimia* 2020; **8(2)**, 189-200.

[17] LDS Nascimento, FIDDM Vieira, V Horácio, FP Marques, MF Rosa, SA Souza, RMD Freitas, DEA Uchoa, SE Mazzeto, D Lomonaco and F Avelino. Tailored organosolv banana peels lignins: Improved thermal, antioxidant and antimicrobial performances by controlling process parameters. *International Journal of Biological Macromolecules* 2021; **181**, 241-252.

[18] E Maulidya, M Kanedi, Y Yulianty and E Ernawiati. The effectiveness of ethanol extract in muli banana peels (*Musa acuminata*) to heal cut wounds in mice (*Mus musculus* L.) (*in Indonesian*). *BIOSFER: Jurnal Tadris Biologi* 2020; **11(1)**, 17-25.

[19] FN Jannah, S Rahayu and N Latifah. Pemanfaatan limbah ekstrak kulit pisang muli (*Musa acuminata* Linn.) sebagai masker *gel peel off* (*in Indonesian*). *Sinteza: Jurnal Farmasi Klinis dan Sains Bahan Alam* 2022; **2(2)**, 67-72.

[20] VFD Amaral, EAD Lago, W Kondo, LCG Souza and JC Francisco. Development of an experimental model of endometriosis in rats. *Revista do Colegio Brasileiro de Cirurgioes* 2009; **36(3)**, 250-255.

[21] BF Eddie-Amadi, AN Ezejiofor, CN Orish, J Rovira, TA Allison and OE Orisakwe. Banana peel ameliorated hepato-renal damage and exerted anti-inflammatory and anti-apoptotic effects in metal mixture mediated hepatic nephropathy by activation of Nrf2/Hmox-1 and inhibition of Nfkb pathway. *Food and Chemical Toxicology* 2022; **170**, 113471.

[22] C Edenta, SIR Okoduwa and O Okpe. Effects of aqueous extract of three cultivars of banana (*Musa acuminata*) fruit peel on kidney and liver function indices in wistar rats. *Medicines* 2017; **4(4)**, 77.

[23] L Zhang, K Mohankumar, G Martin, F Mariyam, Y Park, SJ Han and S Safe. Flavonoids quercetin and kaempferol are NR4A1 antagonists and suppress endometriosis in female mice. *Endocrinology* 2023; **164(10)**, bqad133.

[24] S Park, W Lim, FW Bazer, K Whang and G Song. Quercetin inhibits proliferation of endometriosis regulating cyclin D1 and its target microRNAs *in vitro* and *in vivo*. *The Journal of Nutritional Biochemistry* 2018; **63**, 87-100.

[25] J Zhao, J Wang, J Liu, S Li, P Liu and X Zhang. Effect and mechanisms of kaempferol against endometriosis based on network pharmacology and *in vitro* experiments. *BMC Complementary Medicine and Therapies* 2022; **22**, 254.

[26] S Sutrisno, I Miryani, PM Dwijayasa, NR Suprobo and IWA Wiyasa. Genistein administration increases the level of superoxide dismutase and glutathione peroxidase in the endometriosis mice model: An experimental study. *International Journal of Reproductive Biomedicine* 2022; **20(10)**, 873-882.

[27] G Hongxia, J Xiaojie, L Guangxian, Z Min, N Shiwei, C Wangjie, Z Han, Z Yuanding, L Chenghao, L Yaling, S Yun and L Yongqi. Licoflavone A suppresses gastric cancer growth and metastasis by blocking the VEGFR-2 signaling pathway. *Journal of Oncology* 2022; **2022(1)**, 5497991.

[28] Q Wu, Q Zhou, C Wan, G Xin, T Wang, Y Gao, T Liu, X Yu, B Zhang and W Hang. Mechanism actions of coniferyl alcohol in improving cardiac dysfunction in renovascular hypertension studied by experimental verification and network pharmacology. *International Journal of Molecular Sciences* 2024; **25(18)**, 10063.

[29] DS Bryan, DS Bryan, M Stack, K Krysztofiak, U Cichoń, DG Thomas, A Surcel, ES Schiffhauer, MA Beckett, NN Khodarev, L Xue, EC Poli, AT Pearson, MC Posner, DN Robinson, RS Rock and RR Weichselbaum. 4-Hydroxyacetophenone modulates the actomyosin cytoskeleton to reduce metastasis. *Proceedings of the National Academy of Sciences of the United States of America* 2020; **117(36)**, 22423.

[30] S Yang, L Wang, Y Zeng, Y Wang, T Pei, Z Xie, Q Xiong, H Wei, W Li, J Li, Q Su, D Wei and W Cheng. Salidroside alleviates cognitive impairment by inhibiting ferroptosis via activation of the Nrf2/GPX4 axis in SAMP8 mice. *Phytomedicine* 2023; **114**, 154762.

[31] X Xu, Y Lai and Z Hua. Apoptosis and apoptotic body: Disease message and therapeutic target potentials. *Bioscience Reports* 2019; **39**, BSR20180992.

[32] J Wu, YS Fu, K Lin, X Huang, YJ Chen, D Lai, N Kang, L Huang and CF Weng. A narrative review: The pharmaceutical evolution of phenolic syringaldehyde. *Biomedicine and Pharmacotherapy* 2022; **153**, 113339.

[33] U Baroroh, ZS Muscifa, W Destiarani, FG Rohmatulloh and M Yusuf. Molecular interaction analysis and visualization of protein-ligand docking using Biovia Discovery Studio Visualizer. *Indonesian Journal Of Computational Biology* 2023; **2(1)**, 22-30.

[34] N Misuan, S Mohamad, T Tubiana and MKK Yap. Ensemble-based molecular docking and spectrofluorometric analysis of interaction between cytotoxin and tumor necrosis factor receptor 1. *Journal of Biomolecular Structure and Dynamics* 2023; **41(24)**, 15339-15353.

[35] L Pinzi and G Rastelli. Molecular docking: Shifting paradional in drug discovery. *Journal of Molecular Sciences* 2019; **20(18)**, 4331.

[36] A Hairulazam, IA Samian, AAA Hamid and N Alias. *In silico* docking of epicatechin, corilagin and quercetin as potential pancreatic lipase inhibitor for obesity treatment. *International Journal of Allied Health Sciences* 2021; **5(2)**, 2194-2200.

[37] Y Qu, X Li, F Xu, S Zhao, X Wu, Y Wang and J Xie. Kaempferol alleviates murine experimental colitis by restoring gut microbiota and inhibiting the LPS-TLR4-NF- kB Axis. *Frontiers in Immunology* 2021; **12**, 679897.

[38] S Sutrisno, H Aprina, HM Simanungkalit, A Andriyani, W Barlianto, H Sujuti, S Santoso, PM Dwijayasa, ES Wahyuni and E Mustofa. Genistein modulates the estrogen receptor and suppresses angiogenesis and inflammation in the murine model of peritoneal endometriosis. *Journal of Traditional and Complementary Medicine* 2018; **8(2)**, 278-281.

[39] D Savitri, S Wahyuni, A Bukhari, K Djawad, M Hatta, P Riyanto, B Bahar, S Wahab, F Hamid and Y Rifai. Anti-inflammatory effects of banana (*Musa balbisiana*) peel extract on acne vulgaris: *In vivo* and *in silico* study. *Journal of Taibah University Medical Sciences* 2023; **18(6)**, 1586-1598.

[40] AS Zabala, RA Conforti, MB Delsouc, V Filippa, MM Montt-Guevara, A Giannini, T Simoncini, SS Vallcaneras and M Casais. Estetrol inhibits endometriosis development in an *in vivo* murine model. *Biomolecules* 2024; **14(5)**, 580.

[41] D Ye, Z Li and C Wei. Genistein inhibits the S-phase kinase-associated protein 2 expression in breast cancer cells. *Experimental and Therapeutic Medicine* 2018; **15(1)**, 1069-1075.

[42] J Delenko, X Xue, PK Chatterjee, N Hyman, AJ Shih, RP Adelson, PS Tepes, PK Gregersen and CN Metz. Quercetin enhances decidualization through AKT-ERK-p53 signaling and supports a role for senescence in endometriosis. *Reproductive Biology and Endocrinology* 2024; **22**, 100.

[43] A Chimento, AD Luca, M D'Amico, FD Amicis and V Pezzi. The involvement of natural polyphenols in molecular mechanisms inducing apoptosis in tumor cells: A promising adjuvant in cancer therapy. *International Journal of Molecular Sciences* 2023; **24(2)**, 1680.

[44] J Yu, HL Qi, H Zhang, ZY Zhao, J Zhao and ZY Nie. Morin inhibits dox-induced vascular inflammation by regulating PTEN/AKT/NF-κB pathway. *Inflammation* 2022; **45(6)**, 2406-2418.

[45] WA Barroso, IC Abreu, LS Ribeiro, C Quintino, HPD Souza and TMD Lima. Chemical composition and cytotoxic screening of *Musa*

cavendish green peels extract: Antiproliferative activity by activation of different cellular death types. *Toxicology in Vitro* 2019; **59(9)**, 179-186.

[46] AA Delbandi, M Mahmoudi, A Shervin, S Heidari, R Kolahdouz-Mohammadi and AH Zarnani. Evaluation of apoptosis and angiogenesis in ectopic and eutopic stromal cells of patients with endometriosis compared to non-endometriotic controls. *BMC Women's Health* 2020; **20(1)**, 3.

[47] PA Silva-Pinto, JTCD Pontes, B Aguilar-Morón, CSC Canales, FR Pavan and CA Roque-Borda. Phytochemical insights into flavonoids in cancer: Mechanisms, therapeutic potential, and the case of quercetin. *Heliyon* 2025; **11(4)**, e42682.

[48] L Yu, E Rios, L Castro, J Liu, Y Yan and D Dixon. Genistein: Dual role in women's health. *Nutrients* 2021; **13(9)**, 3048.

[49] P Goleij, M Khandan, MAK Tabari, PM Sanaye, D Alijanzadeh, A Soltani, Z Hosseini, DS Larsen, H Khan, AP Kumar and M Daglia. Unlocking the potential: How flavonoids affect angiogenesis, oxidative stress, inflammation, proliferation, invasion, and alter receptor interactions in endometriosis. *Food Science and Nutrition* 2024; **13(1)**, e4607.

[50] H Situmorang, RL Sutanto, K Tjoa, R Rivaldo and M Adrian. Prevalence and risk factors of primary dysmenorrhoea among medical students: A cross-sectional survey in Indonesia. *BMJ Open* 2024; **14(10)**, e086052.